Published in final edited form as:
J Immunol. 2011 July 15; 187(2): 654–663. doi:10.4049/jimmunol.1003941.

Anti-CD8 antibodies can trigger CD8+ T-cell effector function in the absence of TCR engagement and improve pMHCI tetramer staining

Mathew Clement[*], **Kristin Ladell**[*], **Julia Ekeruche-Makinde**[*], **John J. Miles**[*], **Emily S. J. Edwards**[*], **Garry Dolton**[*], **Tamsin Williams**[*], **Andrea J. A. Schauenburg**[*], **David K. Cole**[*], **Sarah N. Lauder**[*], **Awen M. Gallimore**[*], **Andrew J. Godkin**[*], **Scott R. Burrows**[†], **David A. Price**[*], **Andrew K. Sewell**[*,1], and **Linda Wooldridge**[*,1]

[*]Department of Infection, Immunity and Biochemisty, Henry Wellcome Building, Cardiff University, Heath Park, Cardiff, CF14 4XN, UK

[†]Cellular Immunology Laboratory, Department of Infectious Disease and Immunology, Queensland Institute of Medical Research, Brisbane 4029, Australia

Abstract

CD8+ T-cells recognize immunogenic peptides presented at the cell surface bound to major histocompatibility complex class I (MHCI) molecules. Antigen recognition involves the binding of both T-cell receptor (TCR) and CD8 co-receptor to the same peptide-MHCI (pMHCI) ligand. Specificity is determined by the TCR, whereas CD8 mediates effects on antigen sensitivity. Anti-CD8 antibodies have been used extensively to examine the role of CD8 in CD8+ T-cell activation. However, as previous studies have yielded conflicting results, it is unclear from the literature whether anti-CD8 antibodies *per se* are capable of inducing effector function. Here, we report on the ability of seven monoclonal anti-human CD8 antibodies to activate six human CD8+ T-cell clones with a total of five different specificities. Six out of seven anti-human CD8 antibodies tested did not activate CD8+ T-cells. In contrast, one anti-human CD8 antibody, OKT8, induced effector function in all CD8+ T-cells examined. Moreover, OKT8 was found to enhance TCR/pMHCI on-rates and, as a consequence, could be used to improve pMHCI tetramer staining and the visualization of antigen-specific CD8+ T-cells. The anti-mouse CD8 antibodies, CT-CD8a and CT-CD8b, also activated CD8+ T-cells despite opposing effects on pMHCI tetramer staining. The observed heterogeneity in the ability of anti-CD8 antibodies to trigger T-cell effector function provides an explanation for the apparent incongruity observed in previous studies and should be taken into consideration when interpreting results generated with these reagents. Furthermore, the ability of antibody-mediated CD8-engagement to deliver an activation signal underscores the importance of CD8 in CD8+ T-cell signalling.

Keywords

anti-CD8 antibody; CD8+ T-cell activation; pMHCI tetramer; T-cells; surface plasmon resonance

INTRODUCTION

CD8+ T-cells are essential for the control of viral infection and the natural eradication of cancer. CD8+ T-cells recognize short peptides, 8-13 amino acids in length, presented at the

Correspondence: Linda Wooldridge, Tel: 029 2068 7020, Fax: 029 2068 7007, wooldridgel@cardiff.ac.uk.
[1]LW and AKS contributed equally to this manuscript.

Europe PMC Funders Author Manuscripts

target cell surface bound to major histocompatibility complex class I (MHCI) molecules. T-cell antigen recognition is unique in nature as it involves the binding of a single ligand (peptide-MHC) by two receptors (TCR and coreceptor) (1, 2). The CD8 glycoprotein, which serves as the coreceptor on MHCI-restricted T-cells, acts to enhance the antigen sensitivity of $CD8^+$ T-cells by binding to a largely invariant region of MHCI at a site distinct from the TCR docking platform. CD8 has multiple enhancing effects on early T-cell activation events, including: (i) promotion and stabilization of TCR/pMHCI binding at the cell surface (3-5); (ii) recruitment of essential signalling molecules to the intracellular side of the TCR/CD3/ζ complex (6-11); and, (iii) localization of TCR/pMHCI complexes within specialized membrane micro-domains that act as potentially privileged sites for initiation of the TCR-mediated signalling cascade (12, 13). CD8 binding also controls the level of T-cell crossreactivity (14) and can differentially affect the deployment of $CD8^+$ T-cell effector functions (15).

Anti-CD8 antibodies have been used widely to investigate the role of CD8 in $CD8^+$ T-cell activation. Early studies showed that preincubation with anti-CD8 antibodies can block conjugate formation between effector and target cells (16) and inhibit $CD8^+$ T-cell activation in response to cognate pMHCI presented on the target cell surface (17-20). These findings provided key evidence that CD8 was important in the process of $CD8^+$ T-cell activation. However, considerable heterogeneity between different $CD8^+$ T-cells was apparent in terms of their ability to activate in the presence of anti-CD8 antibodies and, as a result, these reagents were used as tools to classify $CD8^+$ T-cells as either CD8-dependent or CD8-independent (21, 22). Antibody-mediated ligation of T-cell surface molecules, such as CD2, CD3 and CD28 (23, 24), can result in effector function. In contrast, studies of antibody-mediated CD8 ligation in the absence of TCR engagement have yielded conflicting results. Early studies demonstrated that induction of CD8 crosslinking at the cell surface can result in $p56^{lck}$ phosphorylation similar to that seen with anti-CD3 antibodies (25) and elicit downstream effector functions, such as chemokine release (26) and potent cytotoxicity (27). However, in conflict with these data, more recent studies suggest that CD8 ligation alone may actually deliver a negative signal (28, 29).

To date, a cohesive explanation for these widely disparate findings with anti-CD8 antibodies has remained elusive. Furthermore, there has been no systematic study of the effects of multiple different anti-human CD8 antibodies on $CD8^+$ T-cells with different specificities. Here, we report on the ability of a panel of seven monoclonal anti-human CD8 antibodies to induce chemokine/cytokine release and cytotoxicity by six different human $CD8^+$ T-cell clones specific for a total of five different pMHCI antigens. The data, supported by parallel observations in a mouse system, reveal that considerable heterogeneity exists in the ability of anti-CD8 antibodies to activate $CD8^+$ T-cells. These results elucidate the apparent incongruity that has been observed in previous studies and mandate that the disparate effects of anti-CD8 antibodies are considered in the interpretation of results generated with these reagents.

MATERIALS & METHODS

Cells

The following HLA A*0201-restricted $CD8^+$ T-cell clones were used in this study: (i) ILA1, specific for the human telomerase reverse transcriptase (hTERT)-derived epitope ILAKFLHWL (residues 540-548) (30, 31); (ii) ALF3, specific for the influenza A matrix protein (M1)-derived epitope GILGFVFTL (residues 58-66); and, (iii) MEL5 and MEL187.c5, specific for the Melan-A-derived epitope ELAGIGILTV (residues 26-35) (32). The HLA B*0801-restricted $CD8^+$ T-cell clone LC13 is specific for the Epstein-Barr virus (EBV) EBNA3A-derived epitope FLRGRAYGL (residues 339-347) (33), and the HLA

B*3508-restricted $CD8^+$ T-cell clone SB10 is specific for the EBV BZLF1-derived epitope LPEPLPQGQLTAY (residues 52-64) (34). The HLA DR*0101-restricted $CD4^+$ T-cell clone C6 recognizes the influenza A hemagglutinin (HA)-derived epitope PKYVKQNTLKLAT (residues 307-319). $CD8^+$ T-cell lines specific for the EBV BMLF1-derived epitope GLCTLVAML (residues 280-288), restricted by HLA A*0201, were generated as described previously (35). Naïve mouse $CD8^+$ T-cells were obtained by harvesting splenocytes from transgenic F5 mice. A significant percentage of $CD8^+$ T-cells within the splenic population of these mice express the F5 TCR, which recognizes the H-$2D^b$-restricted influenza H17 nucleoprotein-derived epitope ASNENMDAM (36). C1R-A*0201 target cells were generated as described previously (37).

Anti-CD8 antibodies

The following anti-human CD8α antibody clones were used in this study: (i) unconjugated or allophycocyanin-conjugated OKT8 (eBioscience, Hatfield, UK); (ii) unconjugated, fluorescein isothiocyanate (FITC)-conjugated or R-phycoerythrin (PE)-conjugated SK1 (BD Biosciences, Oxford, UK); (iii) unconjugated MCD8 (IqProducts, Groningen, The Netherlands); (iv) unconjugated 32/M4 (Santa Cruz Biotechnology Inc., Heidelberg, Germany); (v) unconjugated C8/144B (Santa Cruz Biotechnology Inc.); and, (vi) allophycocyanin-conjugated DK25 (DAKO, Stockport, UK). The anti-human CD8β antibody clone 2ST8.5H7 was also used, either unconjugated or in PE-conjugated form (Abcam, Cambridge, UK). In functional assays, the maximum possible antibody concentrations were used, determined by the concentration of the commercially available preparation in each case. For experiments with mouse cells, the following unconjugated anti-mouse CD8 antibodies were used: (i) anti-CD8α clone CT-CD8a (Caltag-Medsystems, Buckingham, UK); (ii) anti-CD8α clone 53.6.7 (Biolegend, Cambridge, UK); (iii) anti-CD8β clone KT112 (hybridoma kindly provided by Prof. Rose Zamoyska); and, (iv) anti-CD8β clone CT-CD8b (Caltag-Medsystems).

Generation of OKT8 Fab, $F(ab')_2$ and Fc' fragments

250 μg of the anti-human CD8 antibody OKT8 or the anti-human CD3 antibody OKT3 were digested to yield Fab and Fc' fragments using a Pierce Fab micro-preparation kit (ThermoScientific, Rockford, IL); $F(ab')_2$ fragments were produced similarly using a Pierce $F(ab')_2$ micro-preparation kit (ThermoScientific). IgG fragmentation was performed according to the manufacturer's instructions.

$CD8^+$ T-cell effector function assays

3×10^4 T-cells were mixed with anti-CD8 antibodies at the indicated concentrations, either with or without secondary crosslinking by the addition of 5 μl anti-mouse IgG antibody (Beckman Coulter, High Wycombe, UK), and incubated overnight at 37°C in a 5% CO_2 atmosphere. Positive controls included: (i) target cells pulsed with 10^{-7} M cognate peptide; (ii) 10 μg/ml anti-human CD3 antibody (UCHT1; BD Biosciences); or, (iii) 50 ng/ml phorbol myristate acetate (PMA) and 1 μg/ml ionomycin (Sigma-Aldrich, Dorset, UK). Supernatants were harvested and assayed for MIP1α, MIP1β and RANTES by ELISA (R&D Systems, Abingdon, UK), and for IFNγ, TNFα and IL2 by cytometric bead array (Th1/Th2 kit; BD Biosciences), according to the manufacturer's instructions in each case; mouse MIP1β and IL2 assays were performed by ELISA (R&D Systems). Cytometric bead array (CBA) data were acquired using a FACSCalibur flow cytometer and analyzed with CBA 6 Bead analysis software (BD Biosciences). CD107a mobilization was used to measure T-cell degranulation by flow cytometry as described previously (38). For chromium release assays, 2×10^3 T-cells were treated with anti-CD8 antibodies at the indicated concentrations in 100 μl RPMI1640 medium (Life Technologies, Paisley, UK) supplemented with 100 U/ml penicillin (Life Technologies), 100 μg/ml streptomycin (Life

Technologies), 2mM L-glutamine (Life Technologies) and 2% heat-inactivated fetal calf serum (Life Technologies) (R2 medium). 2×10^3 C1R-A*0201 target cells, labelled with 30 μCi ^{51}Cr (Perkin Elmer, Cambridge, UK) per 10^6 cells for 1 hour previously, were subsequently added. Targets were also cultured alone (target spontaneous release) and with TritonX-100 (Sigma-Aldrich) at a final concentration of 5% (target total release). Cells were incubated at 37°C for 18 hours in a 5% CO_2 atmosphere. For each sample, 20 μl supernatant was harvested and mixed with 150 μl OptiPhase Supermix Scintillation Cocktail (Perkin Elmer). Plates were analyzed using a liquid scintillator and luminescence counter (MicroBeta TriLux; Perkin Elmer) with Microbeta Windows Workstation software (Perkin Elmer). Specific lysis was calculated according to the following formula: (experimental release - target spontaneous release/target total release - target spontaneous release) × 100.

pMHCI tetramer staining and flow cytometry

Soluble biotinylated pMHCI monomers were produced as described previously (3). Tetrameric pMHCI reagents (tetramers) were constructed by the addition of either PE-conjugated streptavidin (Life Technologies) or allophycocyanin-conjugated streptavidin (Prozyme Inc., Hayward, CA) at a pMHCI:streptavidin molar ratio of 4:1. For human $CD8^+$ T-cell clones, 5×10^4 cells were preincubated with anti-CD8 antibody as indicated for 25 minutes on ice, then stained with cognate PE-conjugated tetramer (25 μg/ml) at 37°C for 15 minutes (reviewed in (39)) prior to staining with 5 μl 7-AAD (Viaprobe; BD Biosciences) at 4°C for 30 minutes. For human $CD8^+$ T-cell lines, 5×10^4 cells were preincubated with anti-CD8 antibody as indicated for 25 minutes on ice, then stained with cognate PE-conjugated HLA A*0201 tetramer (25 μg/ml) at 37°C for 15 minutes prior to staining with the amine-reactive fluorescent dye LIVE/DEAD® Fixable Aqua (Life Technologies), Pacific Blue-conjugated anti-human CD14 (clone Tuk4; Caltag-Medsystems), Pacific Blue-conjugated anti-human CD19 (clone SJ25-C1; Caltag-Medsystems), PE-Cy5.5-conjugated anti-human CD4 (clone S3.5; Caltag-Medsystems) and FITC-conjugated anti-human CD8 (clone SK1; BD Biosciences) at 4°C for 20 minutes. For human PBMCs directly *ex vivo*, 1×10^5 cells were preincubated with anti-CD8 antibody as indicated for 25 minutes on ice, then stained with allophycocyanin-conjugated HLA A*0201 tetramer (25 μg/ml) at 37°C for 15 minutes prior to staining with LIVE/DEAD® Fixable Aqua (Life Technologies), Pacific Blue-conjugated anti-human CD14 (clone Tuk4; Caltag-Medsystems), Pacific Blue-conjugated anti-human CD19 (clone SJ25-C1; Caltag-Medsystems), FITC-conjugated anti-human CD3 (clone HIT3a; BD Biosciences), PE-Cy5.5-conjugated anti-human CD4 (clone S3.5; Caltag-Medsystems) and PE-Cy7-conjugated anti-human CD8 (clone RPA-T8; BD Biosciences) at 4°C for 20 minutes. For mouse experiments, 5×10^4 cells were preincubated with 100 μg/ml CT-CD8a (Caltag-Medsystems), 53.6.7 (Biolegend), KT112 (in-house) or CT-CD8b (Caltag-Medsystems) for 25 minutes on ice, then stained with cognate PE-conjugated $H\text{-}2D^b$ tetramer (25μg/ml) at 37°C for 15 minutes prior to staining with LIVE/DEAD® Fixable Aqua (Life Technologies), Pacific Blue-conjugated anti-mouse CD4 (clone RM4-5; BD Biosciences), FITC-conjugated anti-mouse CD45R/B220 (clone RA3-6B2; BD Biosciences) and PerCP-Cy5.5-conjugated anti-mouse CD3 (clone 17A2; BD Biosciences) at 4°C for 20 minutes. Data were acquired using either a FACSCantoII or a modified FACSAriaII flow cytometer (both BD Biosciences) and analyzed with FlowJo software (Tree Star Inc., Ashland, OR).

Intracellular cytokine staining

PBMCs were harvested from a healthy donor and cultured with or without 1 μg/ml phytohemagluttinin (PHA; Alere Ltd., Cheshire, UK) and 25 ng/ml IL15 (Promega, Hampshire, UK) for 7 days, then washed and cultured overnight in R2 medium. 5×10^4 PBMCs (unstimulated or stimulated with PHA/IL15) were resuspended in the presence of 1 μl/ml brefeldin A (GolgiPlug™; Sigma-Aldrich), 0.7 μl/ml monensin (GolgiStop™; BD

Biosciences) and 5 μl/ml anti-CD107a-FITC (clone H4A3; BD Biosciences), then incubated with anti-human CD8 antibodies at the indicated concentrations for 18 hours at 37°C in a 5% CO_2 atmosphere. After washing with PBS, cells were stained with LIVE/DEAD® Fixable Violet (ViViD; Life Technologies), Pacific Blue-conjugated anti-human CD14 (clone Tuk4; Caltag-Medsystems) and Pacific Blue-conjugated anti-human CD19 (clone SJ25-C1; Caltag-Medsystems) at room temperature for 15 minutes. Subsequently, cells were washed and stained with H7-allophycocyanin-conjugated anti-human CD3 (clone SK7; BD Biosciences) and PE-Cy5.5-conjugated anti-human CD4 (clone S3.5; Caltag-Medsystems) at 4°C for 20 minutes, then washed a further three times, resuspended in 200 μl BD Cytofix/Cytoperm™ and incubated at 4°C for 20 minutes. After three additional washes in Perm/Wash™ (BD Biosciences), cells were stained with PE-Cy7-conjugated anti-human IFNγ (clone B27; BD Biosciences), allophycocyanin-conjugated anti-human TNFα (clone MAb11; BD Biosciences) and PE-conjugated anti-human MIP1β (clone D21-1351; BD Biosciences) at 4°C for 20 minutes, washed again three more times and resuspended in 200 μl Perm/Wash™. Data were acquired using a modified FACSAria II flow cytometer (BD Biosciences) and analyzed with FlowJo software (Tree Star Inc.).

Tetramer kinetics experiments

For tetramer association assays, 5×10^5 $CD8^+$ T-cells were washed twice and resuspended in 200 μl PBS with or without anti-human CD8 antibody, then incubated with cognate tetramer (5 μg/ml). At indicated time points, 12 μl of the cell suspension was removed and acquired using a FACSCalibur flow cytometer (BD Biosciences). Data were analyzed using FlowJo software (Tree Star Inc.). Tetramer decay analysis was performed as described previously (3).

Surface plasmon resonance (SPR) analysis

Soluble TCRs derived from the MEL5 and MEL187.c5 $CD8^+$ T-cell clones were manufactured as described previously (40-42). Binding analysis was performed using a BIAcore 3000™ equipped with a CM5 sensor chip (43). Between 200 and 400 response units (RUs) of biotinylated pMHCI was immobilized to streptavidin, which was chemically linked to the chip surface. The pMHCI was injected at a slow flow rate (10 μl/min) to ensure uniform distribution on the chip surface. Combined with the small amount of pMHCI bound to the chip surface, this reduced the likelihood of off-rate limiting mass transfer effects. The MEL5 TCR and MEL187.c5 TCRs were purified and concentrated to ~100 μM on the day of SPR analysis to reduce the likelihood of TCR aggregation affecting the results. For equilibrium analysis, eight serial dilutions were carefully prepared in triplicate for each sample and injected over the relevant sensor chips at 25°C. The TCRs were injected over the chip surface at a flow rate of 45 μl/min. Results were analyzed using BIAevaluation 3.1, Microsoft Excel and Origin 6.1. The equilibrium binding constant (K_D) values were calculated using a nonlinear curve fit ($y = (P_1x)/(P_2 + x)$).

RESULTS

Anti-CD8 antibodies can trigger T-cell effector function in the absence of TCR engagement

Several studies suggest that antibody-mediated ligation of CD8 in the absence of TCR engagement can elicit downstream effector function (25-27); however, others have reported the delivery of negative signals with this manipulation (28, 29). To reconcile these apparently disparate findings, we conducted a systematic study of the effects of multiple different anti-human CD8 antibodies on $CD8^+$ T-cells with several different specificities. For this purpose, we used a panel of anti-human CD8 antibodies that comprised six anti-CD8α antibodies (OKT8, SK1, MCD8, 32/M4, C8/144B and DK25) and one anti-CD8β antibody (2ST8.5H7). Six out of seven anti-human CD8 antibodies from the panel (SK1,

MCD8, 32/M4, C8/144B, DK25 and 2ST8.5H7) did not elicit any chemokine production when incubated with four different HLA A*0201-restricted $CD8^+$ T-cell clones (ILA1, ALF3, MEL5 and MEL187.c5) with a total of three different specificities in the absence of specific pMHCI antigen (Figure 1). However, the anti-CD8α antibody OKT8 induced MIP1α, MIP1β and RANTES release from all four HLA A*0201-restricted $CD8^+$ T-cell clones (Figure 1). Chemokine secretion was apparent over a range of OKT8 concentrations (Figure S1).

In addition, we measured chemokine release by two non-HLA A*0201-restricted $CD8^+$ T-cell clones following incubation with each anti-human CD8 antibody from the panel. Both of these non-HLA A*0201-restricted $CD8^+$ T-cell clones produced MIP1α, MIP1β and RANTES in response to OKT8 but did not activate in the presence of the other antibodies tested (Figure 2). Remarkably, the highly antigen sensitive HLA B*3508-restricted EBV BZLF1-specific $CD8^+$ T-cell clone SB10 released >2000 pg/ml of each chemokine in response to OKT8 (Figure 2B). OKT8 was incapable of staining the HLA DR*0101-restricted $CD4^+$ T-cell clone C6 (Figure S2A) and failed to induce chemokine release from this clone (Figure S2B-D). Thus, the stimulatory effects of OKT8 appear to be $CD8^+$ T-cell-specific.

The panel of seven anti-human CD8 antibodies was further tested in cytotoxicity assays with 4 different $CD8^+$ T-cell clones (MEL187.c5, ALF3, LC13 and SB10). Anti-human CD8 antibodies that were incapable of inducing chemokine release failed to elicit cytotoxic activity in any of these four $CD8^+$ T-cell clones (Figure 3). In contrast, SB10 $CD8^+$ T-cells exhibited substantial cytotoxicity in response to stimulation with OKT8; lower levels of specific lysis were also induced in the $CD8^+$ T-cell clones LC13 (3.18%), ALF3 (5.1%) and MEL187.c5 (3.8%) (Figure 3 and data not shown). These results are consistent with a previous study that described a mouse anti-CD8 antibody, KT112, capable of inducing cytotoxicity (27). Collectively, these data indicate that considerable heterogeneity exists in the ability of anti-CD8 antibodies to activate $CD8^+$ T-cells.

OKT8 induces chemokine secretion in the absence of cytokine secretion

Next, we examined the ability of antibody-mediated CD8 ligation to elicit cytokine release by $CD8^+$ T-cells in the absence of TCR engagement. As expected, the anti-human CD8 antibodies that did not elicit chemokine release or cytotoxic activity (SK1, MCD8, 32/M4, C8/144B, DK25 and 2ST8.5H7) also failed to induce IFNγ, TNFα or IL2 release (Figure 4). Interestingly, OKT8 similarly failed to elicit cytokine production from the majority of $CD8^+$ T-cell clones tested (Figure 4). Importantly, chemokine and cytokine assays were performed using the same supernatant, thereby confirming that OKT8 stimulated $CD8^+$ T-cells to secrete chemokines in the absence of cytokine production; one exception to this dichotomy occurred with the $CD8^+$ T-cell clone SB10, which released IFNγ in response to treatment with OKT8. These data suggest that OKT8-mediated CD8 ligation delivers a signal that falls below the threshold required for cytokine production in most $CD8^+$ T-cells.

Neither secondary antibody crosslinking nor PHA/IL15 treatment alter the functional phenotype of anti-human CD8 antibodies

To probe the possibility that the degree of crosslinking mediated by each of the anti-human CD8 antibodies tested could explain the functional heterogeneity observed between these reagents, we performed activation experiments with the addition of secondary antibodies. Secondary crosslinking of OKT8 increased the level of MIP1α, MIP1β and RANTES release by ILA1, ALF3, MEL5, MEL187.c5, LC13 and SB10 $CD8^+$ T-cells above that observed with OKT8 alone (Figure 5 and data not shown). However, secondary antibody-

mediated crosslinking did not reverse the phenotype of the non-activating anti-human CD8 antibodies (Figure 5).

We also examined the effect of PHA/IL15 treatment on the ability of anti-human CD8 antibodies to elicit effector function from $CD8^+$ T-cells in healthy donor PBMCs. PHA is capable of crosslinking glycosylated proteins at the T-cell surface. The seven anti-human CD8 antibodies tested did not substantially activate $CD8^+$ T-cells in untreated PBMCs (Figure 6A). The six non-activating anti-human CD8 antibodies also failed to induce substantial levels of $CD8^+$ T-cell activation in PBMCs cultured for 7 days in PHA/IL15 (Figure 6B). In contrast, OKT8 activated $CD8^+$ T-cells in PHA/IL15-stimulated PBMCs to release MIP1β and degranulate as measured by surface mobilization of CD107a. Interestingly, OKT8 also induced IFNγ and TNFα production by $CD8^+$ T-cells in PHA/IL15-stimulated PBMCs, thereby suggesting that this treatment regimen synergistically lowered the activation threshold of the responding cells. OKT8 failed to activate $CD4^+$ T-cells in PHA/IL15-stimulated PBMCs (Figure 6C), consistent with previously discussed data (Figure S2).

OKT8 enhances pMHCI tetramer staining

Next, we tested the effects of anti-human CD8 antibodies on the staining of ILA1, ALF3, MEL5 and MEL187.c5 $CD8^+$ T-cells with cognate pMHCI tetramers. Three anti-human CD8 antibody clones (SK1, DK25 and 2ST8.5H7) inhibited tetramer staining; clones MCD8, 32/M4 and C8/144B had little or no effect on staining. However, preincubation with OKT8 enhanced cognate pMHCI tetramer staining of all four $CD8^+$ T-cell clones (Figure 7). Thus, OKT8 can enhance the binding of pMHCI tetramers in a range of systems. These findings suggested that OKT8 might facilitate the identification of antigen-specific $CD8^+$ T-cells within mixed cell populations. To test this idea, we examined pMHCI tetramer staining of $CD8^+$ T-cell lines raised against the HLA A*0201-restricted EBV BMLF1-derived epitope GLCTLVAML (residues 280-288). OKT8 enhanced the staining intensity of cognate $CD8^+$ T-cells with the relevant pMHCI tetramer without concomitant increases in non-cognate HLA A*0201 tetramer binding (Figure 8A&B). No increase in the percentage of $tetramer^+CD8^+$ cells was observed in the presence of OKT8 (Figure 8A&B), which likely reflects the high affinity TCR/pMHCI interactions that characterize antiviral $CD8^+$ T-cell populations (41).

We hypothesized that OKT8-mediated enhancement of TCR/pMHCI binding at the cell surface might have beneficial effects on pMHCI tetramer staining with low affinity ligands, an effect that could prove very useful for the detection of $CD8^+$ T-cells with TCRs that bind weakly to cognate antigen, such as those that appear to predominate in anti-cancer and autoimmune responses (32, 41). To test this hypothesis, we used two monoclonal $CD8^+$ T-cell systems and a series of altered peptide ligands that vary in their affinity for cognate TCR by over 5-fold (Table I & Figure S3). Preincubation with OKT8 enhanced staining efficiency with all variant pMHCI tetramers, including low affinity variants (Table I & Figure S4). Consistent with this finding, OKT8 increased both the staining intensity and the percentage of antigen-specific events detected when $CD8^+$ T-cell lines raised against the HLA A*0201-restricted Melan-A-derived epitope ELAGIGILTV (residues 26-35) were stained with HLA A*0201 tetramers folded around the low affinity peptide variants **F**LAGIGILTV or EL**T**GIGILTV (Figure 8C&D).

OKT8 enhances TCR/pMHCI on-rates at the cell surface

To examine how OKT8 enhances antigen binding at the $CD8^+$ T-cell surface in more detail, we examined the effects of this antibody on TCR/pMHCI kinetics using pMHCI tetramers. Differences in tetramer off-rates were minimal (data not shown). However, pretreatment of

$CD8^+$ T-cells with OKT8 resulted in a significant increase in the TCR/pMHCI on-rate at the cell surface in each $CD8^+$ T-cell clone tested (Figure 9). In contrast, DK25 inhibited pMHCI tetramer binding at the cell surface (Figure 9B). OKT8 antibody-induced enhancement of pMHCI tetramer on-rates was also apparent with CD8-null tetramers (Figure 9C). Collectively, these data indicate that OKT8 enhances pMHCI tetramer staining by increasing the on-rate. Furthermore, OKT8 antibody-mediated augmentation of antigen binding at the cell surface occurs independently of the pMHCI/CD8 interaction.

OKT8 $F(ab')_2$ fragments can enhance tetramer staining and elicit $CD8^+$ T-cell effector function

Antibodies can be digested by papain or pepsin to produce Fab or $F(ab')_2$ fragments, respectively. These enzymatically generated fragments have been used extensively in the past to study the structure and function of antibodies. We examined the ability of OKT8 Fab and $F(ab')_2$ fragments to enhance pMHCI tetramer staining and induce chemokine release in the absence of TCR engagement. Not surprisingly, Fab fragments of OKT8 failed to activate $CD8^+$ T-cells or enhance pMHCI tetramer staining (Figure 10A&B). Interestingly, however, OKT8 $F(ab')_2$ fragments retained some ability to enhance pMHCI tetramer staining and elicit chemokine release (Figure 10A&B). OKT8-mediated effects were diminished by pepsin digestion, but anti-human CD3 antibodies were similarly impaired functionally after digestion with this enzyme (Figure 10C); this latter effect has been described previously (44-46). Thus, it appears that intact OKT8 exerts effects on pMHCI tetramer binding and $CD8^+$ T cell activation more efficiently than derived $F(ab')_2$ fragments. However, cellular activation by OKT8 $F(ab')_2$ fragments confirms that this effect is not entirely Fc'-dependent.

Anti-mouse CD8 antibodies can trigger $CD8^+$ T-cell effector function in the absence of TCR engagement

To extend these findings beyond human systems (summarized in Table II), we examined the effects of the anti-mouse CD8α antibody CT-CD8a and the anti-mouse CD8β antibody CT-CD8b on pMHCI tetramer staining and $CD8^+$ T-cell activation in the absence of TCR engagement. We observed that CT-CD8a inhibited tetramer staining of mouse transgenic F5 $CD8^+$ T-cells, whereas CT-CD8b enhanced tetramer staining of the same antigen-specific population (Figure 11A). These results are consistent with our previous findings (26). Interestingly, despite opposing effects on pMHCI tetramer staining, both of these anti-mouse CD8 antibodies induced MIP1β production in the absence of TCR engagement from both naïve and antigen-exposed F5 $CD8^+$ T-cells (Figure 11B & data not shown). These effects were shown to be CD8-specific and occurred in the absence of any concomitant IL2 release (data not shown). The anti-mouse CD8 antibodies 53.6.7 and KT112 both enhanced pMHCI tetramer staining and induced small amounts of MIP1β production (Figure 11A&B). Thus, three different phenotypes were identified within a panel of four different anti-mouse CD8 antibodies (Table III), which further underscores the considerable heterogeneity that exists within this group of reagents.

DISCUSSION

Anti-CD8 antibodies are integral to the flow cytometric detection of pMHCI-restricted T-cells and have been used extensively in the past to identify an important role for CD8 in $CD8^+$ T-cell activation (16-18, 20). Most studies have concluded that anti-CD8 antibodies inhibit the recognition of cognate antigen (19, 21, 22). Furthermore, a recent study provided evidence that a single anti-CD8 antibody could deliver a negative signal to a $CD8^+$ T-cell clone in the absence of cognate antigen (29). In contrast, however, earlier studies concluded that anti-CD8 antibodies could activate $CD8^+$ T-cells (25, 27). Thus, contradictory effects of antibody-mediated CD8 ligation have been reported and the overall picture remains unclear.

To clarify this issue, we examined the ability of seven different monoclonal anti-human CD8 antibodies to activate six different human $CD8^+$ T-cell clones specific for a total of five different pMHCI antigens.

In the absence of cognate antigen, the anti-human CD8 antibody OKT8 induced chemokine release from all six human $CD8^+$ T-cell clones tested and cytotoxic activity in all four human $CD8^+$ T-cell clones tested (Figures 1, 2 & 3). Interestingly, this activation appeared to occur in the absence of any detectable cytokine release, with the exception of $CD8^+$ T-cell clone SB10, which released IFNγ (Figure 4). It is well established that a hierarchy of $CD8^+$ T-cell effector functions exists with respect to antigen sensitivity (47, 48); thus, each function exhibits a distinct activation threshold that must be exceeded for triggering to occur. Our findings suggest that OKT8 delivers a positive signal to $CD8^+$ T-cells that is generally sufficient to exceed the activation threshold required for chemokine release and cytotoxic activity, but is not sufficient to trigger cytokine release in the majority of $CD8^+$ T-cells. In contrast to OKT8, the anti-human CD8α antibody clones SK1, MCD8, C8/144B, 32/M4 and DK25, and the anti-human CD8β antibody clone 2ST8.5H7, did not induce any measurable T-cell effector functions in the absence of cognate antigen. It was not possible to reverse the phenotype of the non-activating anti-human CD8 antibodies by secondary antibody-mediated crosslinking or PHA/IL15 treatment (Figures 5 & 6). Thus, we conclude that anti-CD8 antibodies can exert differential effects on $CD8^+$ T-cells. These findings help to reconcile disparate observations and suggest that previous reports in the literature may not be intrinsically contradictory, but rather reflective of the considerable heterogeneity that characterizes the ability of anti-CD8 antibodies to induce $CD8^+$ T-cell effector function.

Anti-CD8 antibody-mediated activation of $CD8^+$ T-cells is consistent with a recent report, in which we demonstrated that MHCI molecules with super-enhanced CD8 binding properties can also activate $CD8^+$ T-cells in the absence of a specific TCR/pMHCI interaction (49). Furthermore, thymus leukaemia antigen (TL) interacts strongly (K_D = 12μM) with cell surface CD8αα expressed by intraepithelial lymphocytes (IELs) and can modulate T-cell responses independently of the TCR (50-52). These studies all demonstrate that the engagement of CD8 in the absence of cognate antigen binding to the TCR can activate $CD8^+$ T-cells and, collectively, underscore the importance of CD8 in T-cell signalling.

To examine the effects of OKT8 on antigen binding at the $CD8^+$ T-cell surface, we employed soluble pMHCI tetramer technology, which has transformed the study of antigen-specific $CD8^+$ T-cells by enabling their visualization, enumeration, phenotypic characterization and isolation from *ex vivo* samples. Preincubation with OKT8 enhanced the capture of cognate pMHCI tetramers from solution and produced higher intensity staining (Figures 7, 8 & 9). Accordingly, OKT8 enhanced the identification of $CD8^+$ T-cells with low affinity TCR/pMHCI interactions (Figure 8 & Table I), such as those that typically predominate in tumour-specific and autoimmune responses (41). The other anti-CD8 antibodies examined in this study either exerted inhibitory effects on pMHCI tetramer binding (SK1, DK25 and 2ST8.5H7) or displayed no biologically significant activity in this regard (MCD8, 32/M4 and C8/144B). Thus, OKT8 can be used as a tool to improve pMHCI tetramer staining; this property may be especially useful in the context of low avidity antigen-specific $CD8^+$ T-cell populations.

The findings described above suggest that OKT8 has properties that are distinct from other anti-human CD8 antibodies. Furthermore, these properties are not entirely Fc'-dependent (Figure 10). To extend these results, we conducted additional experiments with the anti-mouse CD8α antibody CT-CD8a and the anti-mouse CD8β antibody CT-CD8b. CT-CD8a was shown to inhibit pMHCI tetramer staining, whereas CT-CD8b enhanced pMHCI tetramer binding, consistent with a previous report (26). Despite their differential effects on

pMHCI tetramer binding, both of these anti-mouse CD8 antibodies activated $CD8^+$ T-cells efficiently (Figure 11). These results demonstrate that the ability of anti-CD8 antibodies to elicit $CD8^+$ T-cell effector function does not always correlate with their effect on pMHCI tetramer staining. This lack of correspondence was further supported by the identification of a third phenotype in the mouse system. The anti-mouse CD8α antibody 53.6.7 and the anti-mouse CD8β antibody KT112 both enhanced pMHCI tetramer staining but only activated $CD8^+$ T-cells weakly (Table III). Taken together, these data further underline the heterogeneity that exists within this group of reagents.

The mechanism by which anti-CD8 antibodies exert either inhibitory or stimulatory effects on pMHCI recognition remains elusive. Previous studies have shown that anti-CD8 antibodies retain their effects in the absence of a pMHCI/CD8 interaction (26, 53-55). Here, we confirm that the enhancing effects of OKT8 on HLA A*0201 tetramer on-rate at the cell surface are still apparent in the context of CD8-null MHCI molecules (Figure 9); thus, these effects are independent of any interaction between pMHCI and CD8. Subtle local re-arrangements of the TCR relative to CD8 on pMHCI engagement are required for optimal $CD8^+$ T-cell activation (56, 57). By extension, it seems likely that anti-CD8 antibodies exert their effects by interfering with, or enhancing, this surface receptor topology. The observation that anti-CD4 antibodies can block cell surface intermolecular interactions essential for calcium flux and inhibit subsequent synapse formation is consistent with this hypothesis (58). Furthermore, we have previously demonstrated that anti-CD4 antibodies can interfere with pMHCII tetramer binding despite the fact that the pMHCII/CD4 interaction does not stabilize TCR/pMHCII interactions (59).

In summary, we have shown that: (i) heterogeneity exists in the ability of anti-CD8 antibodies to activate $CD8^+$ T-cells; (ii) antibody-mediated ligation of CD8 in the absence of TCR engagement can induce chemokine release and cytotoxic activity, largely in the absence of cytokine release; (iii) the anti-human CD8 antibody OKT8 can enhance pMHCI tetramer staining; and, (iv) anti-mouse CD8 antibodies (CT-CD8a and CT-CD8b) can activate $CD8^+$ T-cells in the absence of TCR engagement despite differential effects on pMHCI tetramer staining. Thus, anti-CD8 antibodies can have potent effects on TCR/pMHCI binding kinetics and activation. These effects vary according to the antibody clone under investigation and should be taken into account when interpreting studies using these reagents. Furthermore, the ability of antibody-mediated CD8 engagement to activate $CD8^+$ T-cells underscores the importance of coreceptor function in $CD8^+$ T-cell signalling.

Supplementary Material

Refer to Web version on PubMed Central for supplementary material.

Acknowledgments

We would like to thank Rose Zamoyska for helpful discussions and provision of the KT112 hybridoma. We would also like to thank Katherine Adams for the MEL187.c5 $CD8^+$ T-cell clone.

LW is a Wellcome Trust Clinical Intermediate Fellow; MC and JE-M are also funded by the Wellcome Trust. AKS is funded by the Cardiff University Link Chair scheme. DAP is a Medical Research Council (UK) Senior Clinical Fellow; KL is also funded by the Medical Research Council. DKC is a Leverhulme Trust Early Career Fellow. JJM is supported by a Welsh Office of Research and Development (WORD) Translational Fellowship and a National Health and Medical Research Council (NHMRC) Biomedical Fellowship. SRB is a NHMRC Senior Fellow.

REFERENCES

1. Gao GF, Tormo J, Gerth UC, Wyer JR, McMichael AJ, Stuart DI, Bell JI, Jones EY, Jakobsen BK. Crystal structure of the complex between human CD8alpha(alpha) and HLA-A2. Nature. 1997; 387:630–634. [PubMed: 9177355]
2. Gao GF, Rao Z, Bell JI. Molecular coordination of alphabeta T-cell receptors and coreceptors CD8 and CD4 in their recognition of peptide-MHC ligands. Trends Immunol. 2002; 23:408–413. [PubMed: 12133804]
3. Wooldridge L, van den Berg HA, Glick M, Gostick E, Laugel B, Hutchinson SL, Milicic A, Brenchley JM, Douek DC, Price DA, Sewell AK. Interaction between the CD8 coreceptor and major histocompatibility complex class I stabilizes T cell receptor-antigen complexes at the cell surface. J Biol Chem. 2005; 280:27491–27501. [PubMed: 15837791]
4. Gakamsky DM, Luescher IF, Pramanik A, Kopito RB, Lemonnier F, Vogel H, Rigler R, Pecht I. CD8 kinetically promotes ligand binding to the T-cell antigen receptor. Biophys J. 2005; 89:2121–2133. [PubMed: 15980174]
5. van den Berg HA, Wooldridge L, Laugel B, Sewell AK. Coreceptor CD8-driven modulation of T cell antigen receptor specificity. J Theor Biol. 2007; 249:395–408. [PubMed: 17869274]
6. Veillette A, Bookman MA, Horak EM, Bolen JB. The CD4 and CD8 T cell surface antigens are associated with the internal membrane tyrosine-protein kinase p56lck. Cell. 1988; 55:301–308. [PubMed: 3262426]
7. Barber EK, Dasgupta JD, Schlossman SF, Trevillyan JM, Rudd CE. The CD4 and CD8 antigens are coupled to a protein-tyrosine kinase (p56lck) that phosphorylates the CD3 complex. Proc Natl Acad Sci U S A. 1989; 86:3277–3281. [PubMed: 2470098]
8. Zamoyska R, Derham P, Gorman SD, von Hoegen P, Bolen JB, Veillette A, Parnes JR. Inability of CD8 alpha' polypeptides to associate with p56lck correlates with impaired function in vitro and lack of expression in vivo. Nature. 1989; 342:278–281. [PubMed: 2509945]
9. Chalupny NJ, Ledbetter JA, Kavathas P. Association of CD8 with p56lck is required for early T cell signalling events. Embo J. 1991; 10:1201–1207. [PubMed: 1902413]
10. Purbhoo MA, Boulter JM, Price DA, Vuidepot AL, Hourigan CS, Dunbar PR, Olson K, Dawson SJ, Phillips RE, Jakobsen BK, Bell JI, Sewell AK. The human CD8 coreceptor effects cytotoxic T cell activation and antigen sensitivity primarily by mediating complete phosphorylation of the T cell receptor zeta chain. J Biol Chem. 2001; 276:32786–32792. [PubMed: 11438524]
11. Hutchinson SL, Wooldridge L, Tafuro S, Laugel B, Glick M, Boulter JM, Jakobsen BK, Price DA, Sewell AK. The CD8 T cell coreceptor exhibits disproportionate biological activity at extremely low binding affinities. J Biol Chem. 2003; 278:24285–24293. [PubMed: 12697765]
12. Arcaro A, Gregoire C, Boucheron N, Stotz S, Palmer E, Malissen B, Luescher IF. Essential role of CD8 palmitoylation in CD8 coreceptor function. J Immunol. 2000; 165:2068–2076. [PubMed: 10925291]
13. Arcaro A, Gregoire C, Bakker TR, Baldi L, Jordan M, Goffin L, Boucheron N, Wurm F, van der Merwe PA, Malissen B, Luescher IF. CD8beta endows CD8 with efficient coreceptor function by coupling T cell receptor/CD3 to raft-associated CD8/p56(lck) complexes. J Exp Med. 2001; 194:1485–1495. [PubMed: 11714755]
14. Wooldridge L, Laugel B, Ekeruche J, Clement M, van den Berg HA, Price DA, Sewell AK. CD8 controls T cell cross-reactivity. J Immunol. 2010; 185:4625–4632. [PubMed: 20844204]
15. Laugel B, Price DA, Milicic A, Sewell AK. CD8 exerts differential effects on the deployment of cytotoxic T lymphocyte effector functions. Eur J Immunol. 2007; 37:905–913. [PubMed: 17393387]
16. Norment AM, Salter RD, Parham P, Engelhard VH, Littman DR. Cell-cell adhesion mediated by CD8 and MHC class I molecules. Nature. 1988; 336:79–81. [PubMed: 3263576]
17. Shinohara N, Sachs DH. Mouse alloantibodies capable of blocking cytotoxic T-cell function. I. Relationship between the antigen reactive with blocking antibodies and the Lyt-2 locus. J Exp Med. 1979; 150:432–444. [PubMed: 113478]

18. Nakayama E, Shiku H, Stockert E, Oettgen HF, Old LJ. Cytotoxic T cells: Lyt phenotype and blocking of killing activity by Lyt antisera. Proc Natl Acad Sci U S A. 1979; 76:1977–1981. [PubMed: 88050]
19. Janeway CA Jr. The T cell receptor as a multicomponent signalling machine: CD4/CD8 coreceptors and CD45 in T cell activation. Annu Rev Immunol. 1992; 10:645–674. [PubMed: 1534242]
20. Miceli MC, Parnes JR. Role of CD4 and CD8 in T cell activation and differentiation. Adv Immunol. 1993; 53:59–122. [PubMed: 8512039]
21. MacDonald HR, Glasebrook AL, Bron C, Kelso A, Cerottini JC. Clonal heterogeneity in the functional requirement for Lyt-2/3 molecules on cytolytic T lymphocytes (CTL): possible implications for the affinity of CTL antigen receptors. Immunol Rev. 1982; 68:89–115. [PubMed: 6184308]
22. MacDonald HR, Glasebrook AL, Cerottini JC. Clonal heterogeneity in the functional requirement for Lyt-2/3 molecules on cytolytic T lymphocytes: analysis by antibody blocking and selective trypsinization. J Exp Med. 1982; 156:1711–1722. [PubMed: 6983559]
23. Clark SJ, Law DA, Paterson DJ, Puklavec M, Williams AF. Activation of rat T lymphocytes by anti-CD2 monoclonal antibodies. J Exp Med. 1988; 167:1861–1872. [PubMed: 3133442]
24. Luhder F, Huang Y, Dennehy KM, Guntermann C, Muller I, Winkler E, Kerkau T, Ikemizu S, Davis SJ, Hanke T, Hunig T. Topological requirements and signaling properties of T cell-activating, anti-CD28 antibody superagonists. J Exp Med. 2003; 197:955–966. [PubMed: 12707299]
25. Veillette A, Zuniga-Pflucker JC, Bolen JB, Kruisbeek AM. Engagement of CD4 and CD8 expressed on immature thymocytes induces activation of intracellular tyrosine phosphorylation pathways. J Exp Med. 1989; 170:1671–1680. [PubMed: 2478653]
26. Wooldridge L, Hutchinson SL, Choi EM, Lissina A, Jones E, Mirza F, Dunbar PR, Price DA, Cerundolo V, Sewell AK. Anti-CD8 antibodies can inhibit or enhance peptide-MHC class I (pMHCI) multimer binding: this is paralleled by their effects on CTL activation and occurs in the absence of an interaction between pMHCI and CD8 on the cell surface. J Immunol. 2003; 171:6650–6660. [PubMed: 14662868]
27. Tomonari K, Spencer S. Epitope-specific binding of CD8 regulates activation of T cells and induction of cytotoxicity. Int Immunol. 1990; 2:1189–1194. [PubMed: 1708676]
28. Grebe KM, Clarke RL, Potter TA. Ligation of CD8 leads to apoptosis of thymocytes that have not undergone positive selection. Proc Natl Acad Sci U S A. 2004; 101:10410–10415. [PubMed: 15232005]
29. Abidi SH, Dong T, Vuong MT, Sreenu VB, Rowland-Jones SL, Evans EJ, Davis SJ. Differential remodeling of a T-cell transcriptome following CD8-versus CD3-induced signaling. Cell Res. 2008; 18:641–648. [PubMed: 18475290]
30. Laugel B, van den Berg HA, Gostick E, Cole DK, Wooldridge L, Boulter J, Milicic A, Price DA, Sewell AK. Different T cell receptor affinity thresholds and CD8 coreceptor dependence govern cytotoxic T lymphocyte activation and tetramer binding properties. J Biol Chem. 2007; 282:23799–23810. [PubMed: 17540778]
31. Purbhoo MA, Li Y, Sutton DH, Brewer JE, Gostick E, Bossi G, Laugel B, Moysey R, Baston E, Liddy N, Cameron B, Bennett AD, Ashfield R, Milicic A, Price DA, Classon BJ, Sewell AK, Jakobsen BK. The HLA A*0201-restricted hTERT(540-548) peptide is not detected on tumor cells by a CTL clone or a high-affinity T-cell receptor. Mol Cancer Ther. 2007; 6:2081–2091. [PubMed: 17620437]
32. Cole DK, Edwards ES, Wynn KK, Clement M, Miles JJ, Ladell K, Ekeruche J, Gostick E, Adams KJ, Skowera A, Peakman M, Wooldridge L, Price DA, Sewell AK. Modification of MHC anchor residues generates heteroclitic peptides that alter TCR binding and T cell recognition. J Immunol. 2010; 185:2600–2610. [PubMed: 20639478]
33. Argaet VP, Schmidt CW, Burrows SR, Silins SL, Kurilla MG, Doolan DL, Suhrbier A, Moss DJ, Kieff E, Sculley TB, Misko IS. Dominant selection of an invariant T cell antigen receptor in response to persistent infection by Epstein-Barr virus. J Exp Med. 1994; 180:2335–2340. [PubMed: 7964506]

34. Green KJ, Miles JJ, Tellam J, van Zuylen WJ, Connolly G, Burrows SR. Potent T cell response to a class I-binding 13-mer viral epitope and the influence of HLA micropolymorphism in controlling epitope length. Eur J Immunol. 2004; 34:2510–2519. [PubMed: 15307183]
35. Lissina A, Ladell K, Skowera A, Clement M, Edwards E, Seggewiss R, van den Berg HA, Gostick E, Gallagher K, Jones E, Melenhorst JJ, Godkin AJ, Peakman M, Price DA, Sewell AK, Wooldridge L. Protein kinase inhibitors substantially improve the physical detection of T-cells with peptide-MHC tetramers. J Immunol Methods. 2009; 340:11–24. [PubMed: 18929568]
36. Mamalaki C, Elliott J, Norton T, Yannoutsos N, Townsend AR, Chandler P, Simpson E, Kioussis D. Positive and negative selection in transgenic mice expressing a T-cell receptor specific for influenza nucleoprotein and endogenous superantigen. Dev Immunol. 1993; 3:159–174. [PubMed: 8281031]
37. Wooldridge L, Lissina A, Vernazza J, Gostick E, Laugel B, Hutchinson SL, Mirza F, Dunbar PR, Boulter JM, Glick M, Cerundolo V, van den Berg HA, Price DA, Sewell AK. Enhanced immunogenicity of CTL antigens through mutation of the CD8 binding MHC class I invariant region. Eur J Immunol. 2007; 37:1323–1333. [PubMed: 17429845]
38. Betts MR, Brenchley JM, Price DA, De Rosa SC, Douek DC, Roederer M, Koup RA. Sensitive and viable identification of antigen-specific CD8+ T cells by a flow cytometric assay for degranulation. J Immunol Methods. 2003; 281:65–78. [PubMed: 14580882]
39. Wooldridge L, Lissina A, Cole DK, van den Berg HA, Price DA, Sewell AK. Tricks with tetramers: how to get the most from multimeric peptide-MHC. Immunology. 2009; 126:147–164. [PubMed: 19125886]
40. Li Y, Moysey R, Molloy PE, Vuidepot AL, Mahon T, Baston E, Dunn S, Liddy N, Jacob J, Jakobsen BK, Boulter JM. Directed evolution of human T-cell receptors with picomolar affinities by phage display. Nat Biotechnol. 2005; 23:349–354. [PubMed: 15723046]
41. Cole DK, Pumphrey NJ, Boulter JM, Sami M, Bell JI, Gostick E, Price DA, Gao GF, Sewell AK, Jakobsen BK. Human TCR-binding affinity is governed by MHC class restriction. J Immunol. 2007; 178:5727–5734. [PubMed: 17442956]
42. Cole DK, Yuan F, Rizkallah PJ, Miles JJ, Gostick E, Price DA, Gao GF, Jakobsen BK, Sewell AK. Germ line-governed recognition of a cancer epitope by an immunodominant human T-cell receptor. J Biol Chem. 2009; 284:27281–27289. [PubMed: 19605354]
43. Wyer JR, Willcox BE, Gao GF, Gerth UC, Davis SJ, Bell JI, van der Merwe PA, Jakobsen BK. T cell receptor and coreceptor CD8 alphaalpha bind peptide-MHC independently and with distinct kinetics. Immunity. 1999; 10:219–225. [PubMed: 10072074]
44. Woodle ES, Thistlethwaite JR, Ghobrial IA, Jolliffe LK, Stuart FP, Bluestone JA. OKT3 F(ab')2 fragments--retention of the immunosuppressive properties of whole antibody with marked reduction in T cell activation and lymphokine release. Transplantation. 1991; 52:354–360. [PubMed: 1908148]
45. Herold KC, Burton JB, Francois F, Poumian-Ruiz E, Glandt M, Bluestone JA. Activation of human T cells by FcR nonbinding anti-CD3 mAb, hOKT3gamma1(Ala-Ala). J Clin Invest. 2003; 111:409–418. [PubMed: 12569167]
46. Chatenoud L, Bluestone JA. CD3-specific antibodies: a portal to the treatment of autoimmunity. Nat Rev Immunol. 2007; 7:622–632. [PubMed: 17641665]
47. Valitutti S, Muller S, Dessing M, Lanzavecchia A. Different responses are elicited in cytotoxic T lymphocytes by different levels of T cell receptor occupancy. J Exp Med. 1996; 183:1917–1921. [PubMed: 8666949]
48. Price DA, Sewell AK, Dong T, Tan R, Goulder PJ, Rowland-Jones SL, Phillips RE. Antigen-specific release of beta-chemokines by anti-HIV-1 cytotoxic T lymphocytes. Curr Biol. 1998; 8:355–358. [PubMed: 9512422]
49. Wooldridge L, Clement M, Lissina A, Edwards ES, Ladell K, Ekeruche J, Hewitt RE, Laugel B, Gostick E, Cole DK, Debets R, Berrevoets C, Miles JJ, Burrows SR, Price DA, Sewell AK. MHC class I molecules with Superenhanced CD8 binding properties bypass the requirement for cognate TCR recognition and nonspecifically activate CTLs. J Immunol. 2010; 184:3357–3366. [PubMed: 20190139]

50. Leishman AJ, Naidenko OV, Attinger A, Koning F, Lena CJ, Xiong Y, Chang HC, Reinherz E, Kronenberg M, Cheroutre H. T cell responses modulated through interaction between CD8alphaalpha and the nonclassical MHC class I molecule, TL. Science. 2001; 294:1936–1939. [PubMed: 11729321]
51. Tsujimura K, Obata Y, Kondo E, Nishida K, Matsudaira Y, Akatsuka Y, Kuzushima K, Takahashi T. Thymus leukemia antigen (TL)-specific cytotoxic T lymphocytes recognize the alpha1/alpha2 domain of TL free from antigenic peptides. Int Immunol. 2003; 15:1319–1326. [PubMed: 14565930]
52. Cole DK, Gao GF. CD8: adhesion molecule, co-receptor and immuno-modulator. Cell Mol Immunol. 2004; 1:81–88. [PubMed: 16212893]
53. Van Seventer GA, Van Lier RA, Spits H, Ivanyi P, Melief CJ. Evidence for a regulatory role of the T8 (CD8) antigen in antigen-specific and anti-T3-(CD3)-induced lytic activity of allospecific cytotoxic T lymphocyte clones. Eur J Immunol. 1986; 16:1363–1371. [PubMed: 2430810]
54. Hoo WS, Kranz DM. Role of CD8 in staphylococcal enterotoxin B-mediated lysis by cytotoxic T lymphocytes. J Immunol. 1993; 150:4331–4337. [PubMed: 8482838]
55. Campanelli R, Palermo B, Garbelli S, Mantovani S, Lucchi P, Necker A, Lantelme E, Giachino C. Human CD8 co-receptor is strictly involved in MHC-peptide tetramer-TCR binding and T cell activation. Int Immunol. 2002; 14:39–44. [PubMed: 11751750]
56. Lee PU, Kranz DM. Allogeneic and syngeneic class I MHC complexes drive the association of CD8 and TCR on 2C T cells. Mol Immunol. 2003; 39:687–695. [PubMed: 12531280]
57. Block MS, Johnson AJ, Mendez-Fernandez Y, Pease LR. Monomeric class I molecules mediate TCR/CD3 epsilon/CD8 interaction on the surface of T cells. J Immunol. 2001; 167:821–826. [PubMed: 11441088]
58. Krummel MF, Sjaastad MD, Wulfing C, Davis MM. Differential clustering of CD4 and CD3zeta during T cell recognition. Science. 2000; 289:1349–1352. [PubMed: 10958781]
59. Wooldridge L, Scriba TJ, Milicic A, Laugel B, Gostick E, Price DA, Phillips RE, Sewell AK. Anti-coreceptor antibodies profoundly affect staining with peptide-MHC class I and class II tetramers. Eur J Immunol. 2006; 36:1847–1855. [PubMed: 16783852]

Europe PMC Funders Author Manuscripts

Europe PMC Funders Author Manuscripts

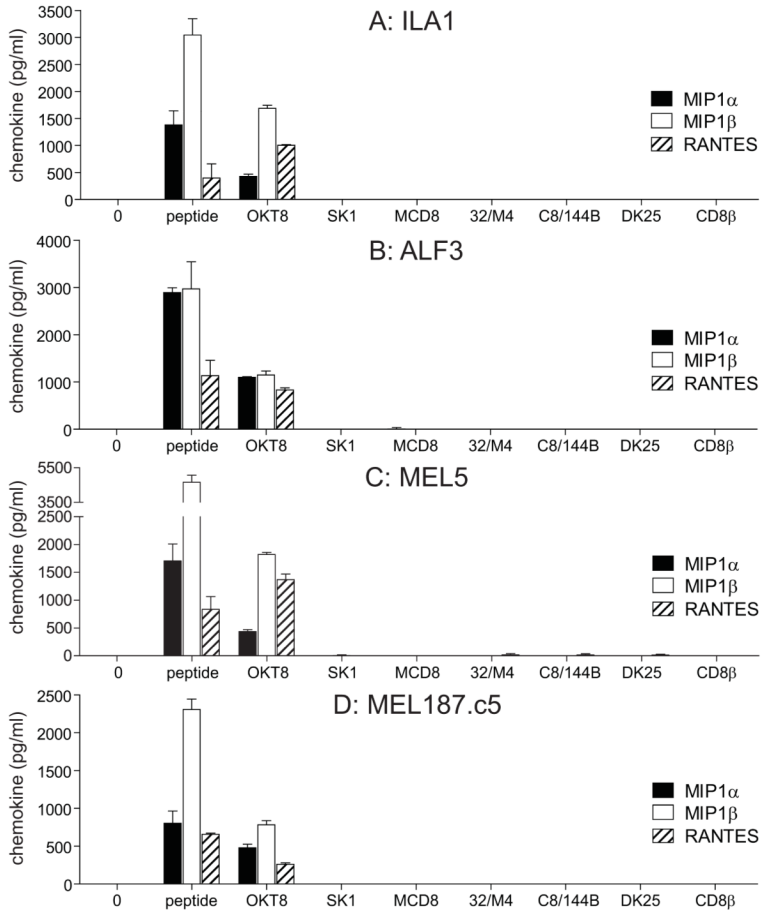

Figure 1. Antibody-mediated CD8 ligation can trigger chemokine release from HLA A*0201-restricted CD8$^+$ T-cells

3×10^4 ILA1 CD8$^+$ T-cells (**A**), ALF3 CD8$^+$ T-cells (**B**), MEL5 CD8$^+$ T-cells (**C**) or MEL187.c5 CD8$^+$ T-cells (**D**) were incubated for 18 hours with each of the following individual anti-human CD8 antibodies in parallel: 100 μg/ml OKT8, 6.25 μg/ml SK1, 50 μg/ml MCD8, 100 μg/ml 32/M4, 100 μg/ml C8/144B, 25 μg/ml DK25 and 100 μg/ml 2ST8.5H7 (CD8β). The maximum possible antibody concentrations were used, determined by the concentration of the commercially available preparation in each case. For each CD8$^+$ T-cell clone, 3×10^4 C1R-A*0201 B-cells pulsed with cognate peptide at 10^{-7} M were used as positive controls. '0' represents T-cells only. Supernatant was harvested and assayed for MIP1α, MIP1β and RANTES by ELISA. Error bars represent standard deviations.

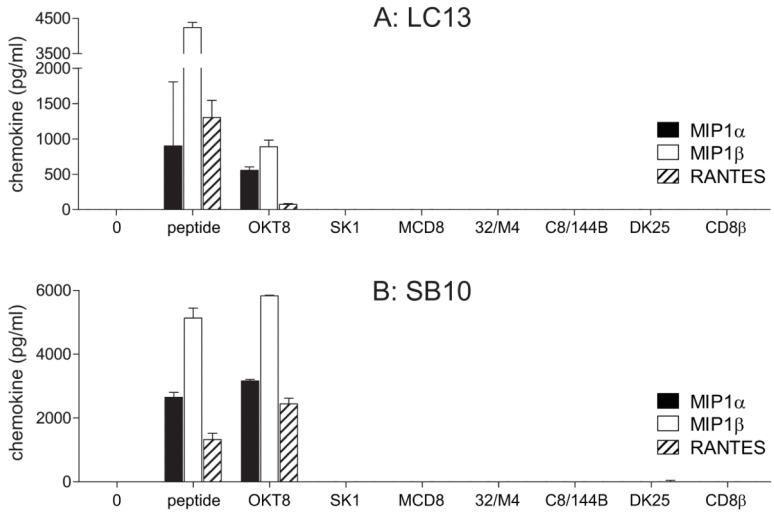

Figure 2. Antibody-mediated CD8 ligation can trigger chemokine release from non-HLA A*0201-restricted CD8$^+$ T-cells

3×10^4 LC13 CD8$^+$ T-cells (**A**) or SB10 CD8$^+$ T-cells (**B**) were incubated for 18 hours with each of the following individual anti-human CD8 antibodies in parallel: 100 μg/ml OKT8, 6.25 μg/ml SK1, 50 μg/ml MCD8, 100 μg/ml 32/M4, 100 μg/ml C8/144B, 25 μg/ml DK25 and 100 μg/ml 2ST8.5H7 (CD8β). For each CD8$^+$ T-cell clone, 3×10^4 HLA-matched B-cells pulsed with cognate peptide at 10^{-7} M were used as positive controls. Supernatant was harvested and assayed for MIP1α, MIP1β and RANTES by ELISA. Error bars represent standard deviations.

Europe PMC Funders Author Manuscripts

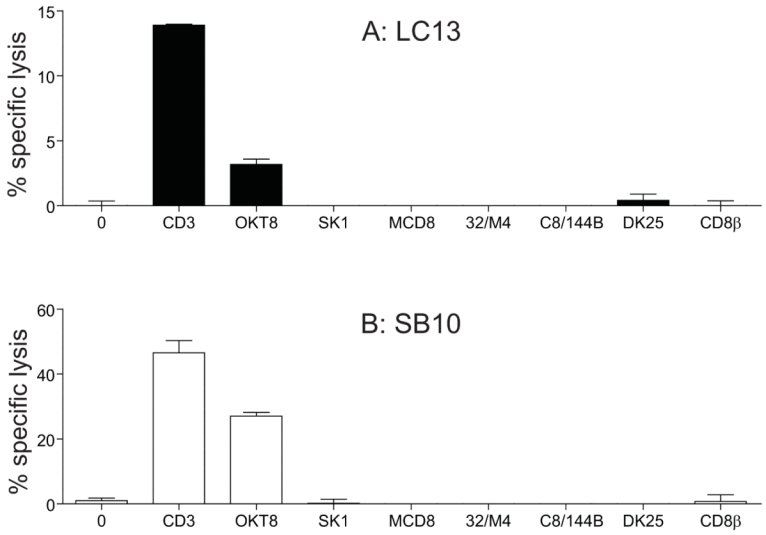

Figure 3. The anti-human CD8 antibody OKT8 can trigger cytotoxic activity

2×10^3 LC13 $CD8^+$ T-cells (**A**) or SB10 $CD8^+$ T-cells (**B**) were incubated with each of the following individual anti-human CD8 antibodies in parallel: 100 μg/ml OKT8, 6.25 μg/ml SK1, 50 μg/ml MCD8, 100 μg/ml 32/M4, 100 μg/ml C8/144B, 25 μg/ml DK25 and 100 μg/ml 2ST8.5H7 (CD8β). The anti-human CD3 antibody UCHT1 (10 μg/ml) served as a positive control. Cytotoxicity assays were then performed over a period of 18 hours as described in the Materials & Methods using ^{51}Cr-labelled C1R-A*0201 B-cells as targets. Error bars represent standard deviations.

Europe PMC Funders Author Manuscripts

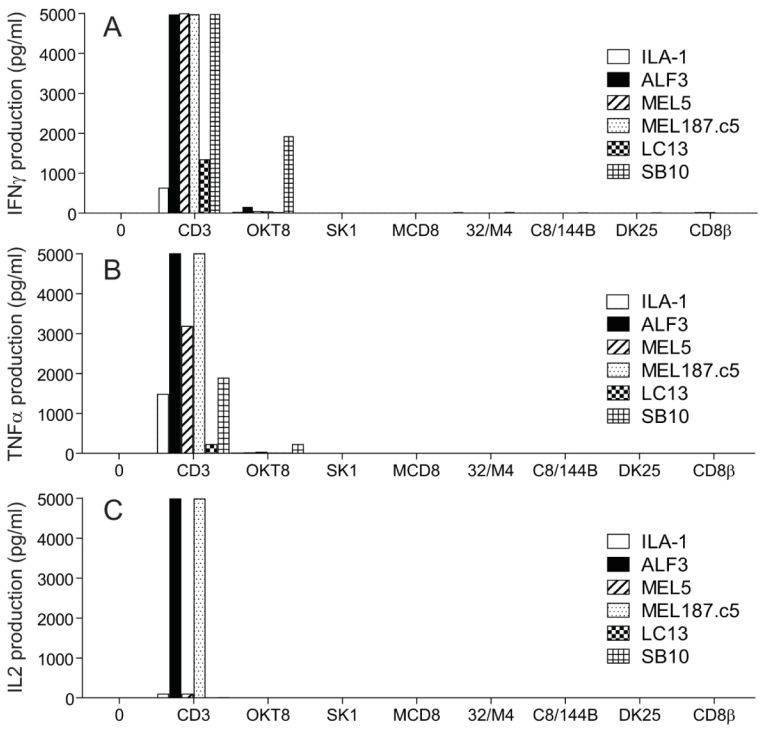

Figure 4. Anti-CD8 antibody-mediated chemokine release occurs in the absence of cytokine release

3×10^4 ILA1, ALF3, MEL5, MEL187.c5, LC13 or SB10 $CD8^+$ T-cells were incubated for 18 hours with each of the following individual anti-human CD8 antibodies in parallel: 100 μg/ml OKT8, 6.25 μg/ml SK1, 50 μg/ml MCD8, 100 μg/ml 32/M4, 100 μg/ml C8/144B, 25 μg/ml DK25 and 100 μg/ml 2ST8.5H7 (CD8β). The anti-human CD3 antibody UCHT1 (10 μg/ml) served as a positive control. Supernatant was harvested and assayed for IFNγ (**A**), TNFα (**B**) and IL2 (**C**) by CBA.

Europe PMC Funders Author Manuscripts

Europe PMC Funders Author Manuscripts

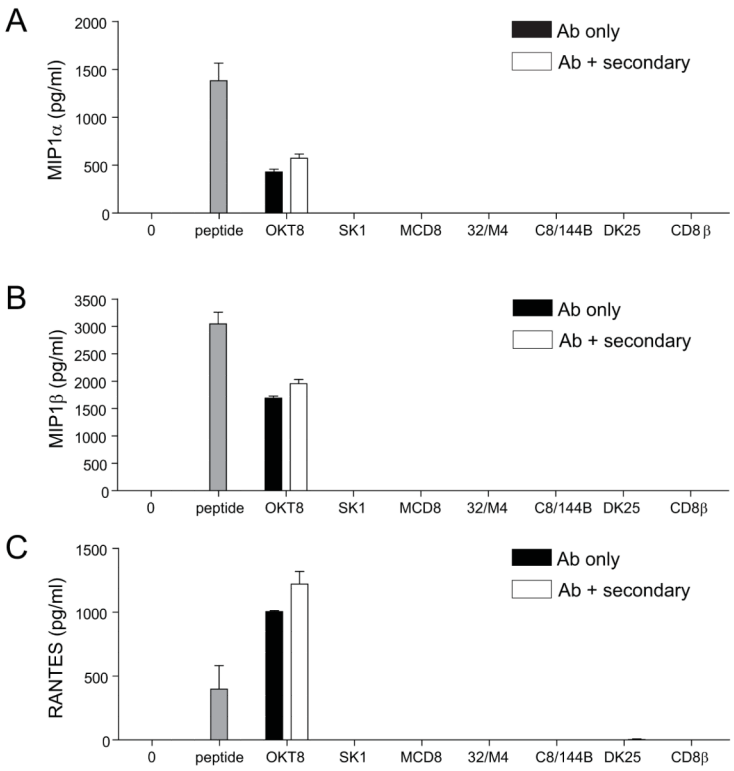

Figure 5. Secondary crosslinking does not alter the functional phenotype of anti-human CD8 antibodies

3×10^4 ILA1 $CD8^+$ T-cells were incubated with each of the following individual anti-human CD8 antibodies in parallel: 100 μg/ml OKT8, 6.25 μg/ml SK1, 50 μg/ml MCD8, 100 μg/ml 32/M4, 100 μg/ml C8/144B, 25 μg/ml DK25 and 100 μg/ml 2ST8.5H7 (CD8β). The positive control comprised 3×10^4 C1R-A*0201 B-cells pulsed with cognate peptide at 10^{-7} M. Antibodies were then crosslinked with the addition of 5 μl anti-mouse IgG antibody (serum IgG) and incubated for 18 hours at 37°C in a 5% CO_2 atmosphere. Supernatant was harvested and assayed for MIP1α (**A**), MIP1β (**B**) and RANTES (**C**) by ELISA. Secondary crosslinking of OKT8 increased the levels of all analytes measured; this also applied to anti-CD3 antibody-induced chemokine release (data not shown). Similar results were obtained with all other $CD8^+$ T-cell clones tested: ALF3, MEL5, MEL187.c5, LC13 and SB10 (data not shown). Error bars represent standard deviations.

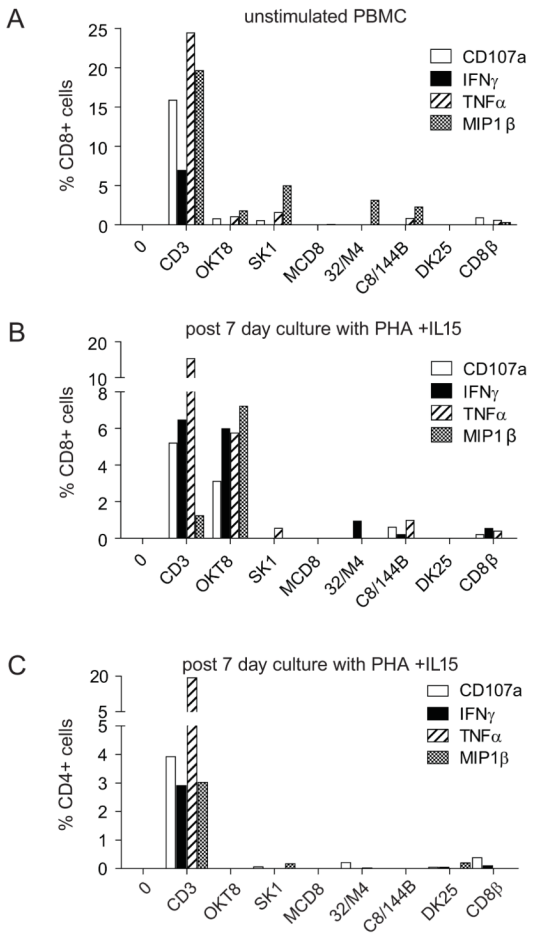

Figure 6. PHA/IL15 treatment does not alter the functional phenotype of anti-human CD8 antibodies

PBMCs were harvested from healthy donors and cultured either without (**A**) or with (**B&C**) 1 μg/ml PHA and 25 ng/ml IL15 for 7 days, then washed and cultured overnight in R2 medium. 5×10^4 PBMCs were then incubated for 18 hours with each of the following individual anti-human CD8 antibodies in parallel: 100 μg/ml OKT8, 6.25 μg/ml SK1, 50 μg/ml MCD8, 100 μg/ml 32/M4, 100 μg/ml C8/144B, 25 μg/ml DK25 and 100 μg/ml 2ST8.5H7 (CD8β). The anti-human CD3 antibody UCHT1 (10 μg/ml) served as a positive control. $CD8^+$ T-cell effector functions were measured by intracellular cytokine staining and surface CD107a mobilization as described in the Materials & Methods. Data were acquired using a modified FACSAriaII flow cytometer and analyzed with FlowJo software. Results obtained by gating on either the $CD3^+CD4^-$ (**A&B**) or $CD4^+$ (**C**) population are shown for a representative experiment (n=2). Minor differences in background levels of $CD8^+$ T-cell activation were observed with the non-OKT8 anti-human CD8 antibodies (**A&B**); this may reflect heterogeneity within the $CD8^+$ PBMC population.

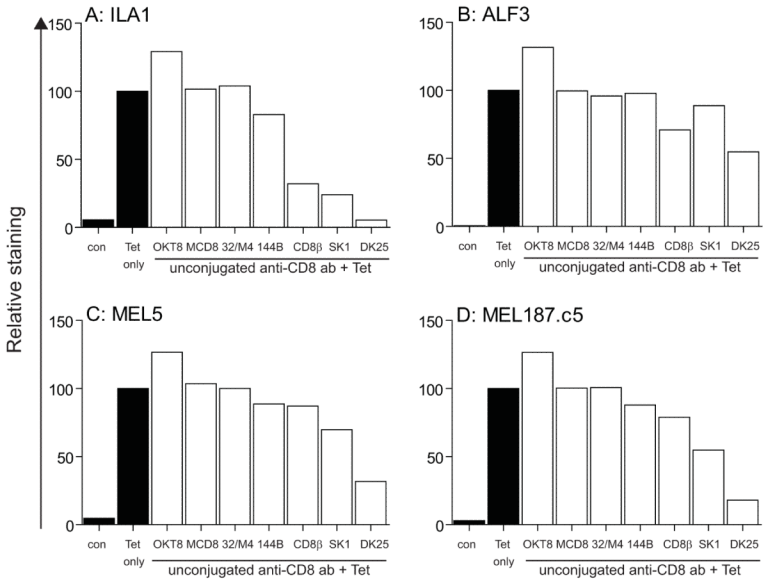

Figure 7. Anti-human CD8 antibodies can either enhance or inhibit the binding of pMHCI tetramers

5×10^4 ILA1 (**A**), ALF3 (**B**), MEL5 (**C**) or MEL187.c5 (**D**) $CD8^+$ T-cells were preincubated at 4°C for 25 minutes with each of the following individual anti-human CD8 antibodies in parallel: 100 μg/ml OKT8, 6.25 μg/ml SK1, 50 μg/ml MCD8, 100 μg/ml 32/M4, 100 μg/ml C8/144B (144B), 25 μg/ml DK25 and 100 μg/ml 2ST8.5H7 (CD8β). $CD8^+$ T-cells were subsequently stained with cognate PE-conjugated HLA A*0201 tetramers (25 μg/ml) and 7-AAD as described in the Materials & Methods. Data were acquired using a FACSCalibur flow cytometer and analyzed with FlowJo software. Relative MFI values with respect to pMHCI tetramer staining in the absence of preincubation with anti-CD8 antibody are shown. Fluorescence in the absence of added cognate tetramer (con) is shown in each case. Data are representative of four separate experiments using ILA1 and ALF3 $CD8^+$ T-cells, and six separate experiments using MEL5 and MEL187.c5 $CD8^+$ T-cells.

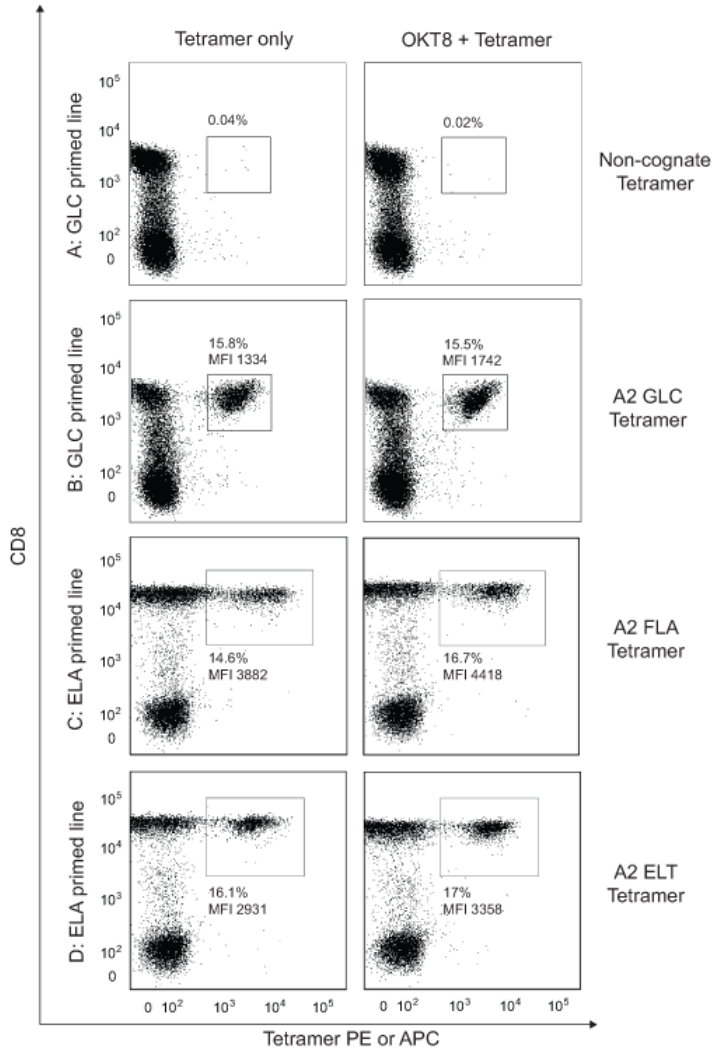

Figure 8. OKT8 enhances pMHCI tetramer staining in mixed cell populations

(**A&B**) 5×10^4 cells from a $CD8^+$ T-cell line primed with the EBV BMLF1-derived epitope GLCTLVAML (residues 280-288) were either mock treated or incubated with 100 μg/ml OKT8 at 4°C for 25 minutes, then stained with either non-cognate HLA A*0201-ELAGIGILTV (**A**) or cognate HLA A*0201-GLCTLVAML (**B**) PE-conjugated tetramer (25μg/ml each) at 37°C for 15 minutes. (**C&D**) 5×10^4 cells from a $CD8^+$ T-cell line primed with the Melan-A-derived epitope ELAGIGILTV (residues 26-35) were either mock treated or incubated with 100 μg/ml OKT8 at 4°C for 25 minutes, then stained with either HLA A*0201-**F**LAGIGILTV (**C**) or HLA A*0201-EL**T**GIGILTV (**D**) PE-conjugated tetramer (25μg/ml each) at 37°C for 15 minutes. Additional stains were performed as detailed in the Materials & Methods. Data were acquired using a FACSCantoII flow cytometer and analyzed with FlowJo software.

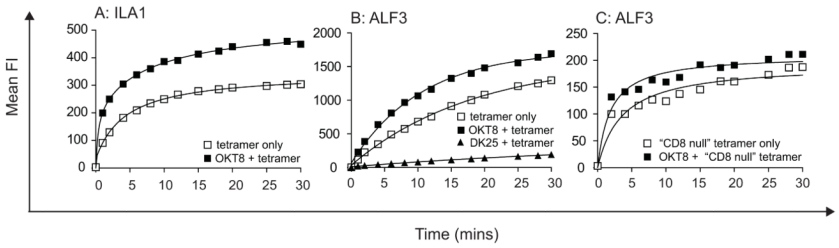

Figure 9. OKT8 increases TCR/pMHCI on-rates at the cell surface

5×10^5 ILA1 (**A**) or ALF3 (**B&C)** $CD8^+$ T-cells were removed from culture, washed twice and resuspended in 100 μl PBS with or without 100 μg/ml OKT8 or 25 μg/ml DK25, then incubated at 4°C for 25 minutes. Cognate PE-conjugated HLA A*0201 tetramer was added in each case at 5 μg/ml. At various time points as indicated, 12 μl of cell suspension was removed and analyzed using a FACSCalibur flow cytometer with FlowJo software. In panel (**C**), the CD8-null (D227K/T228A) cognate HLA A*0201 tetramer was used (10).

Europe PMC Funders Author Manuscripts

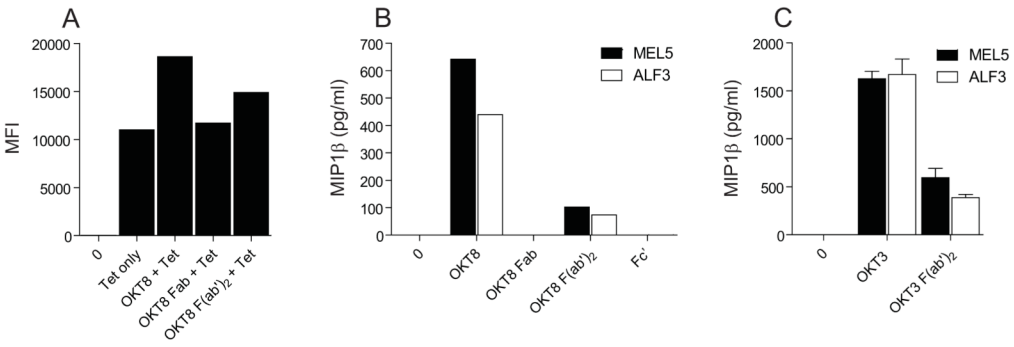

Figure 10. OKT8 F(ab')$_2$ fragments can enhance pMHCI tetramer staining and elicit CD8$^+$ T-cell effector function

(**A**) 5 × 10^4 MEL5 CD8$^+$ T-cells were either mock treated or incubated with 100 μg/ml OKT8, 100 μg/ml OKT8 Fab or 100 μg/ml OKT8 F(ab')$_2$, then stained with PE-conjugated HLA A*0201-ELAGIGILTV tetramer (25 μg/ml) as described in the Materials & Methods. Data were acquired using a FACSCantoII flow cytometer and analyzed with FlowJo software. (**B**) 3×10^4 MEL5 or ALF3 CD8$^+$ T-cells were incubated with either 100 μg/ml OKT8, 100 μg/ml OKT8 Fab, 100 μg/ml OKT8 F(ab')$_2$ or 100 μg/ml OKT8 Fc' for 18 hours. Supernatant was harvested and assayed for MIP1α, MIP1β and RANTES by ELISA. (**C**) 3×10^4 MEL5 or ALF3 CD8$^+$ T-cells were incubated with either 10 μg/ml OKT3 or 10 μg/ml OKT3 F(ab')$_2$ for 18 hours. Supernatant was harvested and assayed for MIP1α, MIP1β and RANTES by ELISA (only MIP1β is shown). Data in **A-C** are representative of three separate experiments. Error bars represent standard deviations.

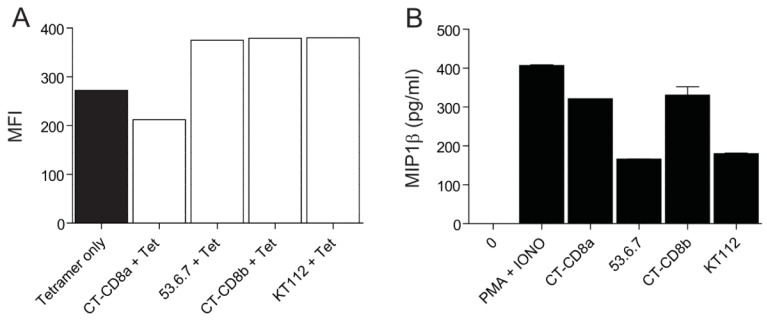

Figure 11. Anti-mouse CD8 antibodies can exhibit the same phenotype as OKT8

(**A**) 5×10^4 naïve mouse transgenic F5 T-cells were either mock treated or incubated with 100 μg/ml CT-CD8a, 100 μg/ml 53.6.7, 100 μg/ml CT-CD8b or 100 μg/ml KT112 at 4°C for 25 minutes, then stained with cognate PE-conjugated H-2D^b tetramer (25μg/ml) as described in the Materials & Methods. No staining was observed under any of the conditions shown with a control H-2D^b tetramer folded around the lymphocytic choriomeningitis virus GP1-derived epitope KAVYNFATC (residues 33-41). Data were acquired using a modified FACSAriaII flow cytometer and analyzed with FlowJo software. Results were obtained by gating on the $CD3^+CD4^-$ population. (**B**) 3×10^4 naïve mouse transgenic F5 T-cells were incubated at 37°C for 18 hours with either 100 μg/ml CT-CD8a, 100 μg/ml 53.6.7, 100 μg/ml CT-CD8b, 100 μg/ml KT112 or PMA (50 ng/ml) and ionomycin (1 μg/ml). Supernatants were harvested and assayed for MIP1β by ELISA. Error bars represent standard deviations.

Europe PMC Funders Author Manuscripts

Table I

OKT8 increases tetramer staining of MEL5 and MEL187.c5 CD8$^+$ T-cells with low affinity pMHCI ligands

Summary of equilibrium binding analysis of MEL5 and MEL187.c5 TCRs with pMHCI variants, and the effect of OKT8 on HLA A*0201 tetramer staining. Raw SPR data are shown in Figure S3; flow cytometry data are shown in Figure S4. MFI, median fluorescence intensity.

Peptide	MEL5 K_D (μM)	MEL5 Tetramer only (MFI)	MEL5 OKT8 + Tetramer (MFI)	MEL187 K_D (μM)	MEL187 Tetramer only (MFI)	MEL187 OKT8 + Tetramer (MFI)
ELAGIGILTV	17 ± 1	855	917	18 ± 1	353	418
FLAGIGILTV	92 ± 1	194	227	30 ± 2	300	373
EL**T**GIGILTV	82 ± 4	36	87	37 ± 1	128	181
ELAGIGI**I**TV	77 ± 3	123	236	36 ± 3	195	257
FLAGIGI**I**TV	75 ± 3	367	426	47 ± 2	246	311

Europe PMC Funders Author Manuscripts

Table II

The heterogeneity of anti-human CD8 antibodies

Summary of the effects exerted by anti-human CD8 antibodies on pMHCI tetramer binding and $CD8^+$ T-cell activation in the absence of TCR engagement.

Ab Clone	α or β	Tetramer binding	MIP1β	MIP1α	RANTES	IFNγ	TNFα	IL2	Cyto toxicity
OKT8	α	Enhance	Yes	Yes	Yes	No*	No*	No	Yes
SK1	α	Inhibit	No	No	No	No	No	No	No
MCD8	α	Neutral	No	No	No	No	No	No	No
32/M4	α	Neutral	No	No	No	No	No	No	No
C8/144B	α	Neutral	No	No	No	No	No	No	No
DK25	α	Inhibit	No	No	No	No	No	No	No
2ST8.5H7	β	Inhibit	No	No	No	No	No	No	No

*OKT8 was shown to elicit IFNγ and TNFα release by SB10 and PHA/IL15-stimulated PBMC.

Europe PMC Funders Author Manuscripts

J Immunol. Author manuscript; available in PMC 2012 January 15.

Table III

The heterogeneity of anti-mouse CD8 antibodies

Summary of the effects exerted by anti-mouse CD8 antibodies on pMHCI tetramer binding and $CD8^+$ T-cell activation in the absence of TCR engagement.

Ab Clone	α or β	Tetramer binding	MIP1β	IFNγ	IL2
CT-CD8a	α	Inhibit	Yes	No	No
53.6.7	α	Enhance	Weak *	No	No
CT-CD8b	β	Enhance	Yes	No	No
KT112	β	Enhance	Weak	NT	NT

* 53.6.7 elicited low levels of MIP1β production from naïve F5 $CD8^+$ T-cells, F5 $CD8^+$ T-cell lines and blasted BALB/c $CD8^+$ cells, but not from naive BALB/c $CD8^+$ cells (data not shown). NT, not tested.